EPJ E
Soft Matter and Biological Physics
EPJ.org
your physics journal

Eur. Phys. J. E (2011) **34**: 57 DOI: 10.1140/epje/i2011-11057-0

The stability of solitons in biomembranes and nerves

B. Lautrup, R. Appali, A.D. Jackson and T. Heimburg

EDP SCIENCES
Società Italiana di Fisica
Springer

Eur. Phys. J. E (2011) **34**: 57
DOI 10.1140/epje/i2011-11057-0

THE EUROPEAN PHYSICAL JOURNAL E

Regular Article

The stability of solitons in biomembranes and nerves

B. Lautrup[a], R. Appali, A.D. Jackson, and T. Heimburg[b]

Niels Bohr Institute, Blegdamsvej 17, DK-2100, Copenhagen Ø, Denmark

Received 3 September 2010 and Received in final form 3 March 2011
Published online: 9 June 2011 –

Abstract. We examine the stability of a class of solitons, obtained from a generalization of the Boussinesq equation, which have been proposed to be relevant for pulse propagation in biomembranes and nerves. These solitons are found to be stable with respect to small-amplitude fluctuations. They emerge naturally from non-solitonic initial excitations and are robust in the presence of dissipation. Solitary waves pass through each other with only minor dissipation when their amplitude is small. Large-amplitude solitons fall apart into several pulses and small-amplitude noise upon collision when the maximum density of the membrane is limited by the density of the solid phase membrane.

1 Introduction

The action potential in nerves is a propagating voltage pulse across the axonal membrane with an amplitude of about 100 mV. In 1952, A.L. Hodgkin and A.F. Huxley proposed a model for the nerve pulse which has since become the textbook model [1]. Their picture is based on the equilibration of ion gradients across the nerve membrane through specific ion-conducting proteins (called ion channels) which leads to transient voltage changes. Hodgkin-Huxley model thus relies on dissipative processes and is intrinsically not isentropic. It is rather based on Kirchhoff circuits involving capacitors (the nerve membrane), resistors (the ion channels) and electrical currents introduced by the ion fluxes.

In a series of recent publications we have proposed an alternative thermodynamic model in which nerve pulses are described as a localized density pulse (soliton) in the axon membrane [2–6]. This model allows us to consider a number of issues which are not addressed by the Hodgkin-Huxley model. These include the reversible temperature and heat changes observed in connection with the nerve pulse, which suggest that an isentropic process is responsible for the action potential [7–9]. Further, it naturally predicts the correct pulse propagation velocities in myelinated nerves as these are closely related to the lateral sound velocities in the nerve membrane. The presence of empirically known lipid phase transitions slightly below physiological temperatures is central to our model. The closer the phase transition is to physiological temperatures, the easier it is to excite the nerve pulse. The model therefore immediately explains another interesting feature of nerve excitation, *i.e.*, that the nerve pulse can be induced by a sudden cooling of the nerve, and that it can be inhibited by a temperature increase [10]. The generation of a voltage pulse with compression is merely a consequence of the piezo-electric nature of the nerve membrane, which is partially charged and asymmetric. Our model does not contain ion channel proteins explicitly but rather assumes that their effects are embodied in empirically known macroscopic thermodynamic observables. We note, however, that under the conditions necessary for solitons to propagate, *i.e.*, close to phase transitions in the membrane, fluctuations in pure lipid membrane lead to ion-channel-like events that are virtually indistinguishable from the quantized current events conventionally ascribed to ion channel proteins [11–15]. Their creation is a consequence of the same thermodynamic laws that dictate the properties of the solitons. We have also argued that the thermodynamic nature of the soliton model permits a simple and quantitative description of the action of anesthetics and its dependence on changes in intensive variables (such as hydrostatic pressure) like their familiar effects on the phase transition temperature [3,16].

A primary virtue of a thermodynamic description of pulse propagation in nerves lies in its predictive power. This is a natural consequence of the fact that thermodynamics allows us to establish connections between macroscopic thermodynamic observables without the need for detailed consideration of their microscopic origins. For example, given measured values of the compression modulus as a function of lateral density and frequency, soliton properties (including its shape and its energy) can be determined as a function of soliton velocity with no freely adjustable parameters.

Simple physical arguments lead to an equation appropriate for the description of pulse propagation in mem-

[a] e-mail: lautrup@nbi.dk
[b] e-mail: theimbu@nbi.dk

branes. As we shall see, this equation has strong similarities to the Boussinesq equation [17] and leads to exponentially localized pulses that propagate with a constant shape and a constant velocity. For readers less familiar with the work of Joseph Boussinesq and solitons in general, a few historical remarks may be useful. In 1872 Boussinesq offered a theoretical description of the "*les belles expériences*" of John Scott Russell and Henry Émile Bazin which provided quantitative measurements of the solitary waves first observed by Russell in 1834. In dimensionless form, Boussinesq's equation reads

$$\partial_{tt} f = \partial_x[(1+f)\partial_x f] + \partial_{xxxx} f. \tag{1}$$

Using elementary mathematical techniques he found simple solutions to this equation. With the boundary condition that f should vanish at spatial infinity, these solutions have the form

$$f(x,t) = 3(v^2-1)\,\mathrm{sech}^2\left[\sqrt{v^2-1}(x-vt)/2\right], \tag{2}$$

with $v > 1$. The real significance of this and other solitonic equations was not generally appreciated until the development of more powerful mathematical tools by, *e.g.*, Peter Lax, Martin Kruskal and their co-workers in the 1960s (for an introduction to the mathematics of solitons, see [18]). In particular, if multisoliton solutions were constructed it was recognized that, in spite of the strong interaction between them, "solitons 'pass through' one another without losing their identity" [19] (as we shall see below, the solitary waves considered here do not have this property.) Solitons are now recognized as important in virtually all areas of physics. In addition to their intrinsic mathematical interest, solitons play an important role in hydrodynamics (see above), in quantum field theory [20], antiferromagnetism [21], Bose-Einstein condensates [22,23], nonlinear optics [24–26] and biological systems (DNA) [27,28]. The vast soliton literature also includes many variants of Boussinesq's original equation. (This is due in part to the fact that the dispersion relation for small-amplitude oscillations of eq. (1), $\omega^2 = k^2 - k^4$, suggests short wavelength instabilities and has led to its designation as the "bad Boussinesq equation".) To the best of our knowledge, the variant considered here has not been studied previously.

In [2–6] the possibility of soliton propagation was explored and compared to observations in real nerves. In the present paper we study some intrinsic properties of these solitons, in particular the stability of such pulses in the presence of noise and dissipation. Such investigations are necessary to demonstrate that these pulses can propagate under realistic physiological conditions over the length scales of nerves (as much as several meters) even in the presence of viscosity and lateral inhomogeneities. In the following section, we will state the model more precisely and present the analytic form of its solitonic solutions. We then turn to a description of the numerical methods used here. We use these methods to probe i) the stability of solitons with respect to "infinitesimal" perturbations (*i.e.*, lattice noise), ii) the way in which solitons are produced by localized non-solitonic initial excitations of the system, iii) the behavior of solitons in the presence of dissipation, and iv) head-on collisions of solitons. We will demonstrate that the solitons of ref. [2] are remarkably robust with respect to all of these perturbations. Our approach to these issues is based on elementary analytical methods and numerical calculations. This reflects the fact that our interest here is physical rather than mathematical.

2 Analytic considerations

Thermodynamic measurements of the lipids of biological membranes reveal a number of interesting features of potential relevance for understanding the nature of pulses in biomembranes and nerves. In particular, such systems display an order-disorder transition at temperatures somewhat below that of biological interest from a low-temperature "solid-ordered" phase to a high-temperature "liquid-disordered" phase in which both the lateral order and chain order of the lipid molecules is lost [29]. The proximity of this phase transition to temperatures of biological interest has striking effects on the compression modulus and, hence, on the sound velocity [30,31]. For densities some 10% above the equilibrium density (which is the density of the disordered membrane slightly above the transition corresponding to the resting state of the nerve membrane under physiological conditions), the low-frequency sound velocity is reduced by roughly a factor of 3 from the velocity of $c_0 = 176.6\,\mathrm{m/s}$ found at equilibrium. The sound velocity then rises sharply, returning to the value c_0 at a density roughly 20% above the equilibrium density. Measurements at high frequencies (*i.e.*, 5 MHz) reveal a much smaller dip in the lateral compression modulus and a sound velocity that is always materially larger than that at low frequencies and thus indicate the presence of significant dispersion [31,32].

In ref. [2], these features were exploited to suggest that the propagation of sound in these lipid mixtures can be described by the equation

$$\frac{\partial^2}{\partial\tau^2}\Delta\rho^A = \frac{\partial}{\partial z}\left[\left(c_0^2 + p\Delta\rho^A + q(\Delta\rho^A)^2\right)\frac{\partial}{\partial z}\Delta\rho^A\right] - h\frac{\partial^4}{\partial z^4}\Delta\rho^A. \tag{3}$$

Here, $\Delta\rho^A = \rho^A - \rho_0^A$ is the difference between the lateral mass density of the membrane and its empirical equilibrium value of $\rho_0^A = 4.035 \times 10^{-3}\,\mathrm{g/m^2}$, and the low-frequency sound velocity is $c_0 = 176.6\,\mathrm{m/s}$. The coefficients p and q were fitted to measured values of the sound velocity as a function of density. Although high-frequency sound velocity measurements indicate that the dispersive coefficient, h, must be positive, neither the magnitude of h nor the specific form of this term have been verified experimentally. Note that the sign of the dispersive term is opposite to that familiar from the Boussinesq and Korteweg-de Vries equations. In practice, the only role of h is to establish the linear size of solitons, and it can thus be chosen, *e.g.*, so that the width of the soliton is comparable to that

known for nerve pulses. Here, we choose to work with the dimensionless variables u, x and t defined as

$$u = \frac{\Delta\rho^A}{\rho_0^A}\,,\ x = \frac{c_0}{\sqrt{h}}z\,,\ t = \frac{c_0^2}{\sqrt{h}}\tau,\ B_1 = \frac{\rho_0}{c_0^2}p,\ B_2 = \frac{\rho_0^2}{c_0^2}q. \tag{4}$$

With this choice of variables, eq. (3) assumes the form

$$\frac{\partial^2 u}{\partial t^2} = \frac{\partial}{\partial x}\left(B(u)\frac{\partial u}{\partial x}\right) - \frac{\partial^4 u}{\partial x^4}\,, \tag{5}$$

with

$$B(u) = 1 + B_1 u + B_2 u^2. \tag{6}$$

The qualitative features of the empirical compression modulus require that $B_1 < 0$ and $B_2 > 0$. In the numerical work described below, we will adopt the parameter values $B_1 = -16.6$ and $B_2 = 79.5$ found in ref. [2]. Equation (5) can be recognized as a generalization of the Boussinesq equation, and it is known to have exponentially localized "solitonic" solutions which propagate without distortion for a finite range of sub-sonic velocities. We now determine the analytic form of these solitons.

Since we seek solutions which propagate without distortion, we regard u as a function of $\xi = x - \beta t$ and rewrite eq. (5) as

$$\beta^2\frac{\partial^2 u}{\partial \xi^2} = \frac{\partial}{\partial \xi}\left(B(u)\frac{\partial u}{\partial \xi}\right) - \frac{\partial^4 u}{\partial \xi^4}\,. \tag{7}$$

With the assumption that u vanishes at spatial infinity, we can integrate this equation to yield

$$\left(\frac{\partial u}{\partial \xi}\right)^2 = (1-\beta^2)u^2 + \frac{1}{3}B_1 u^3 + \frac{1}{6}B_2 u^4. \tag{8}$$

The solution will grow from 0 until it reaches a maximum value at which $\partial u/\partial\xi = 0$. Equation (8) then implies that u is symmetric about its maximum value. It also indicates that this is possible only if

$$1 > |\beta| > \beta_0 = \sqrt{1 - \frac{B_1^2}{6B_2}}\,. \tag{9}$$

The minimum velocity β_0 corresponds to the maximum-amplitude solitons. Its numerical value is about 100 m/s [2] and should correspond to the velocity of the nerve pulse above threshold excitation. For the parameters $B_1 = -16.6$ and $B_2 = 79.5$ adopted in [2], we find $\beta_0 \approx 0.649851$. We will use these parameter values in the remainder of this paper.

We thus expect localized solutions for $\beta_0 < |\beta| < 1$. When this condition is met, the right side of eq. (8) will have two real roots, $u = a_\pm$, with

$$a_\pm = -\frac{B_1}{B_2}\left(1 \pm \sqrt{\frac{\beta^2 - \beta_0^2}{1-\beta_0^2}}\right). \tag{10}$$

It is readily verified that the desired solitonic solutions of eq. (5) have the analytic form

$$u(\xi) = \frac{2a_+a_-}{(a_+ + a_-) + (a_+ - a_-)\cosh\left(\xi\sqrt{1-\beta^2}\right)}\,. \tag{11}$$

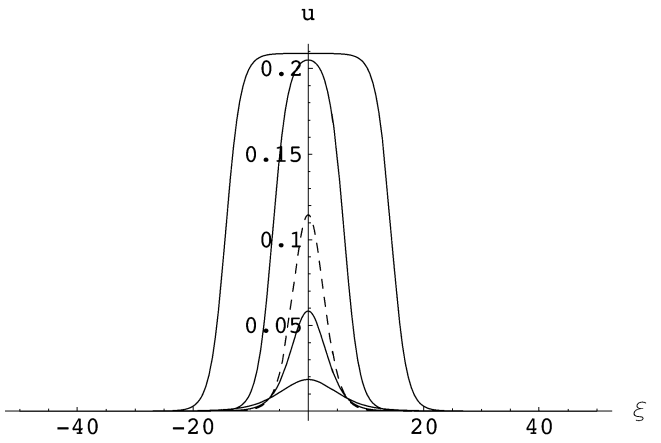

Fig. 1. Soliton profiles for velocities $\beta = \beta_0 + 4\times10^{-9}$, 0.65, 0.734761, 0.85, and 0.95. The maximum height diminishes as a function of β. The width of the soliton diverges for both $\beta \to \beta_0$ and $\beta \to 1$ and has a minimum at $\beta \approx 0.734761$, which corresponds to the dashed curve.

These solutions are shown in fig. 1 for a selection of soliton velocities.

As expected, eq. (5) can be obtained from a suitable energy density. We thus seek an energy density, $\mathcal{E}$, such that eq. (5) will result from variation of the corresponding Lagrangian density. To this end, it is useful to introduce the dimensionless displacement, $s(x,t)$, defined as $u = \partial s/\partial x$. The energy density can then be written as

$$\mathcal{E} = \frac{1}{2}\left(\frac{\partial s}{\partial t}\right)^2 + \left[\frac{1}{2}u^2 A(u) + \frac{1}{2}\left(\frac{\partial u}{\partial x}\right)^2\right], \tag{12}$$

with

$$A(u) = 1 + \frac{1}{3}B_1 u + \frac{1}{6}B_2 u^2. \tag{13}$$

The integral of this energy density over all space is conserved and independent of time. The two terms in eq. (12) represent the kinetic and potential energy densities, respectively. The corresponding Lagrangian density is obtained by changing the sign of the potential energy term, and eq. (5) follows by standard variational arguments. This form of the energy density leads to two important observations. First, we note that the energy density simplifies considerably if u describes a soliton and is given by eq. (11). Specifically, use of the equation of motion allows us to write the energy density as $\mathcal{E}_{\rm sol} = u^2 A(u)$. The specific form of eq. (11) is sufficiently simple that the energy of a soliton can be calculated analytically and involves only elementary functions.

It is also useful to consider the total energy associated with an arbitrary solution, $u(x,t)$, of eq. (5) as given by the integral over all space of the energy density, $\mathcal{E}$, of eq. (12). Recognizing perfect differentials when they arise and making use of the equation of motion, eq. (5), we find the expected result that the energy is independent of time for an arbitrary choice of $u(x,t)$. (This result assumes either that $u(x,t)$ vanishes as $|x| \to \infty$ or that it satisfies periodic boundary conditions in x.) It is also useful to

consider the time dependence of the integral of u over all space,

$$U = \int u(x,t)\,\mathrm{d}x. \tag{14}$$

It is clear from the equation of motion that $\partial^2 U/\partial t^2$ can be expressed as an integral of perfect differentials. Hence, $\partial^2 U/\partial t^2 = 0$ if u vanishes at spatial infinity or is periodic. Thus, the time dependence of U is elementary and can include only a constant term and a term linear in t. As we shall see below, U is independent of time when $u(x,t)$ is periodic.

3 Numerical results

We would like to investigate a number of questions associated with the stability of the solitons of eq. (11). Although the simplicity of the analytic form of these solitons suggests that it may be possible to solve the problem of infinitesimal stability analytically, we have elected to consider this problem numerically. To this end, it is convenient to re-write eq. (5) as two first-order equations. We obtain

$$\frac{\partial u}{\partial t} = \frac{\partial v}{\partial x}\,, \qquad \frac{\partial v}{\partial t} = \frac{\partial f}{\partial x}\,, \tag{15}$$

with

$$f = u + \frac{1}{2}B_1 u^2 + \frac{1}{3}B_2 u^3 - \frac{\partial w}{\partial x}\,, \tag{16}$$

where $w = \partial u/\partial x$ (and incidentally $v = \partial s/\partial t$). The first of eqs. (15) ensures that the spatial integral of u is independent of time if v is chosen to be periodic. Equations (15) are well suited to numerical solution using a variant of the two-step Lax-Wendroff method [33]. This algorithm is both fast and stable in practice. For periodic boundary conditions and the choice of spatial step size $\Delta x = 0.1$ and time step $\Delta t = 0.001$, used below, it was possible to follow 10^6 time steps without discernible loss of accuracy. Note that the energy of eq. (12) is not rigorously conserved by this numerical algorithm. In the following numerical examples, the energy was found to decrease at a roughly constant rate proportional to Δx^2. This fact was used to make an appropriate choice of $\Delta x = 0.1$. The corresponding value of $\Delta t = 0.001$ was selected to yield full numerical stability.

3.1 Small-amplitude perturbations

Our primary numerical concern is to study the stability of the solitonic solutions of eq. (11) with respect to "infinitesimal" perturbations. We employ the parameters $B_1 = -16.6$ and $B_2 = 79.5$ adopted in [2], for which $\beta_0 \approx 0.650$. We will show results for an initial soliton with velocity $\beta = \beta_1 \approx 0.735$. This soliton has a width (*i.e.*, full width at half-maximum) of roughly 6.24, which is the minimum width possible for the values of B_1 and B_2 considered. There is, of course, no reason to believe that a soliton on a discrete lattice with finite Δx will have a profile identical to the analytic form of eq. (11). The use of this analytic form in establishing the initial values of u and v thus inevitably introduces small-amplitude perturbations into the numerical system. Since there is no other "natural" choice for the initial form of the solitonic excitation, this disturbance represents the best approximation to infinitesimal perturbations that can be realized in a numerical study.

In an analytic approach to the question of infinitesimal stability, one considers the time evolution of the sum of the soliton under investigation and a small excitation, $\delta u(x,t) = \psi(x,t)$. The equation of motion (5) is then expanded to first order in ψ, and expressed in terms of t and $\xi = x - \beta t$,

$$\frac{\partial^2\psi}{\partial t^2} - 2\beta\frac{\partial^2\psi}{\partial t\partial\xi} + \beta^2\frac{\partial^2\psi}{\partial\xi^2} = \frac{\partial^2(B(u)\psi)}{\partial\xi^2} - \frac{\partial^4\psi}{\partial\xi^4}\,. \tag{17}$$

It follows that solutions to this (non-Hermitian) equation can be written as the product of functions $\psi_\lambda(\xi)$ and $\exp(\lambda t)$. If one or more of the resulting values of λ has a positive real part, the corresponding $\psi_\lambda(x,t)$ will grow exponentially with time, and the initial solitonic solution will be locally unstable. Since it is our aim to detect precisely such exponential instabilities (if present), it is of no consequence that the numerical perturbation introduced by the finite mesh size is small. Exponential instabilities will be apparent if they are present. The finite size of Δx also means that there is a smallest wavelength perturbation which can be studied on the lattice. In practice, potential instabilities involving such wavelengths will be invisible to numerical studies only if they are orthogonal to those wavelengths which *can* be investigated reliably with the Δx chosen. While this is not impossible, it is unlikely.

Results were obtained with $\Delta x = 0.1$ and $\Delta t = 0.001$. The spatial lattice was chosen to be periodic with length 100. For $\beta = \beta_1 \approx 0.735$, the exact energy of the soliton is 0.0377. The energy of this initial state is smaller by 1.5×10^{-6} when calculated on the lattice. Energy is not strictly conserved by the numerical algorithm adopted but rather decreases linearly with time over the time intervals considered. In the present case, energy is lost at the rate of 7.3×10^{-9} per unit time. We have followed this soliton for times as long as 1000 units, during which the soliton can propagate more than 100 times its own width. The energy loss is negligible, and there is absolutely no indication of instability. (Note that the discrepancy in the initial energy is proportional to Δx^2; the rate of energy loss scales like Δx^3. This expectation has been verified by numerical calculations (data not shown).)

We can illustrate soliton stability in the following manner. We first determine the location of the maximum of the soliton as a function of time. The constancy of its velocity over large time intervals provides an initial indication of the stability of the soliton. In the present case, this velocity is found to be stable and roughly 0.02% less than the initial velocity of the analytic soliton. (This error scales with Δx^2.) There are, of course, small fluctuations in the location of both the maximum density and, hence, the

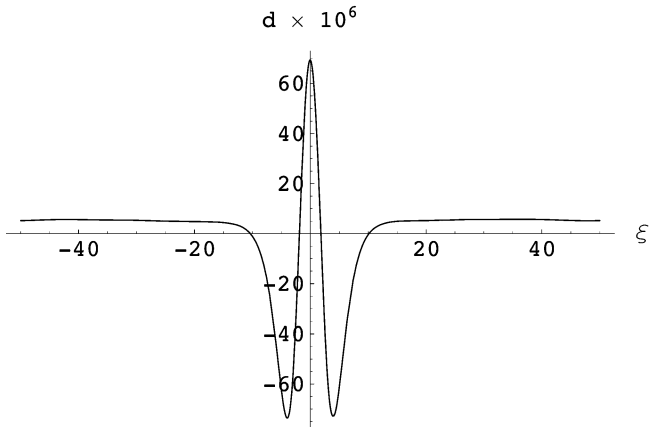

Fig. 2. The difference $d(\xi)$ between the time-averaged numerical soliton and the analytic soliton for the minimum width soliton with $\beta = \beta_1 \approx 0.735$. The average has been performed over 1000 units of time, during which the soliton travels more than 100 times its own width.

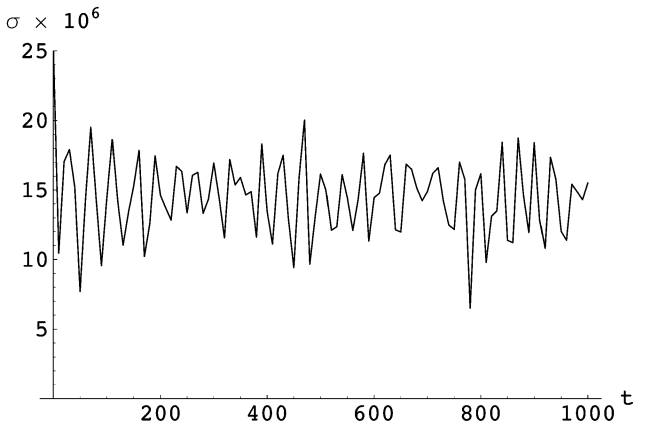

Fig. 3. Time evolution of r.m.s. noise level σ for the minimal width soliton over 1000 units of time.

velocity due to the perturbations. For the present example, such fluctuations in the location of the maximum are never greater than 0.004, which is 25 times smaller than Δx. (These fluctuations also scale like Δx^2.) Having identified the position of soliton as a function of time, each time frame is shifted to locate the soliton at a common point. A time-averaged soliton is then constructed in order to minimize the effects of the perturbations. The difference between the time-averaged soliton and the analytic soliton is shown in fig. 2. The peak value of the time-averaged soliton is slightly (*i.e.*, roughly 0.05%) higher than that of the analytic soliton, and it is somewhat narrower than its analytic counterpart. (The size of these differences again scales with Δx^2.) This demonstrates the claim that the analytic solitons are not identical to solitons on a finite mesh.

We now consider the effects of this perturbation as a function of time by subtracting the time-averaged soliton from the full $u(x,t)$ at each time update and constructing the root mean square of the resulting difference as a function of time. If the soliton is stable, the resulting r.m.s. difference should be bounded as a function of time. If the soliton were unstable, however, we would expect to find systematic differences in the vicinity of the soliton maximum which grow exponentially with time. The spatial distribution of the r.m.s. difference at later times shows no sign of such systematic effects, and its magnitude is the same both near and far from the location of the soliton. The calculated r.m.s. difference is shown in fig. 3 as a function of time. Again, there is no sign of such instabilities. Since qualitatively similar results are found for other values of β, we conclude that the solitons of eq. (5) are stable with respect to small perturbations.

It is also possible to study soliton stability in the presence of larger-amplitude noise. This is most easily done by choosing a form of $u(x,0)$ which consists of both the (analytic) soliton of interest and a linear combination of the lowest $k \leq K$ periodic waves on the interval L, $a_k \sin(2\pi kx/L + \phi_k)$, with phases chosen at random and amplitudes chosen at random subject to a constraint on the overall r.m.s. noise level at $t = 0$. The analysis proceeds as above. We have considered the case of $K = 10$ with an initial r.m.s. noise as large as 5% of the maximum amplitude of the soliton. The results are similar to those found for small-amplitude noise: There are no indications of soliton instability.

3.2 Soliton genesis

It is also instructive to consider finite-amplitude disturbances and to see how a localized but non-solitonic initial state evolves with time. To illustrate this, we choose $u(x,0)$ to be the minimum width soliton of eq. (11). In this case, however, we distort the second initial condition and choose $v(x,0) = -p\,\beta u(x,0)$, with $p = 0.5$. Thus, the initial field is *not* solitonic. The time evolution shows that this initial pulse "sheds" matter and changes its shape through the emission of a smaller soliton, which moves in the opposite direction, and small-amplitude waves, which run ahead of the solitons with velocity $\beta \approx 1$. The two solitons are captured in fig. 4 at $t = 50$. The velocity of the larger soliton is $\beta = 0.799$ and its maximum is at $x = 39.515$ whereas the smaller has $\beta = -0.948$ and maximum at $x = -47.129$. The shape of each of these solitons is accurately described using eq. (11) with the corresponding measured velocity. These two solitons account for virtually all of the initial energy of the system; approximately 0.3% of this energy is associated with the small-amplitude motion distinct from the solitons. In fig. 5 the two solitons have been subtracted out, and only the difference is plotted. This confirms that the shapes are indeed solitonic.

Similar results have been obtained for other non-solitonic initial pulse forms (*e.g.*, Gaussian pulses). In short, for the cases explored, non-solitonic initial excitations evolve into solitons and small-amplitude non-solitonic disturbances. In infinite space, dispersion ensures that the solitonic and non-solitonic components will become spatially distinct and that the amplitude of the latter will decrease with time. This is obviously not the case for the periodic lattice considered here.

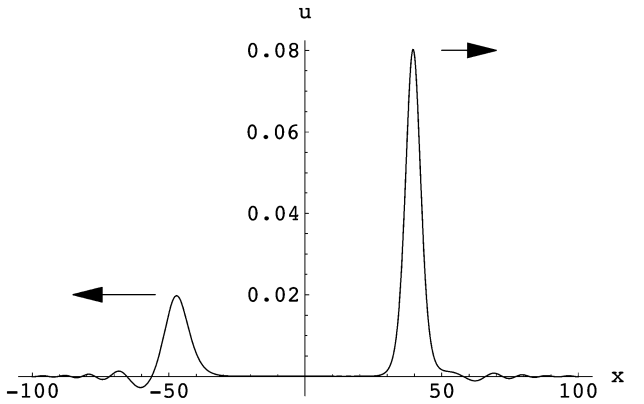

Fig. 4. A minimal width soliton with an initial velocity, β, 50% lower than the corresponding analytic value, shown at $t = 50$. It has divided into two solitons of different sizes, propagating in opposite directions. Small-amplitude waves run ahead of the solitons with velocity $\beta \approx 1$; the region between the solitons is essentially noise free (see also fig. 5). Note that the length of the periodic lattice has been increased here to avoid interference effects between the solitons and the leading small-amplitude waves.

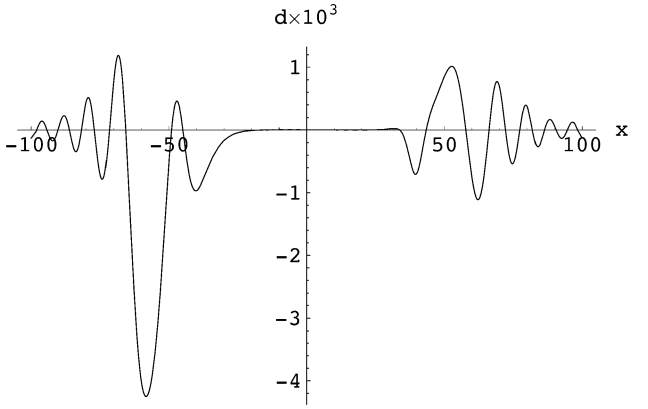

Fig. 5. The graph in fig. 4 with the two solitons subtracted out to leave only the small-amplitude waves running ahead of the solitons.

3.3 Solitons and dissipation

It is also possible to consider the consequences of dissipation on soliton propagation.

The inclusion of viscosity in the Navier-Stokes velocity results in an additional term on the right of eq. (5) of the form $\kappa\partial^3 u/\partial x^2\partial t$ (for derivation see appendix A). This term is readily incorporated in our numerical approach by the inclusion of the term $+\kappa\partial v/\partial\xi$ in eq. (16). We have performed numerical studies with the value $\kappa = 0.05$. With this choice of κ, the height of the soliton is reduced by roughly 70% at $t = 990$ and has travelled more than 100 times its initial width. As energy is dissipated, the soliton accelerates, and its profile changes with the expected drop in its amplitude. Over the entire time range considered, we find that the soliton profile is consistent with the analytic soliton profile of eq. (11) appropriate for the corresponding instantaneous velocity of the pulse. This is illustrated in fig. 6, which shows the comparison of analytic solitons (in infinite space) and these numerical results including dissipation at several times.

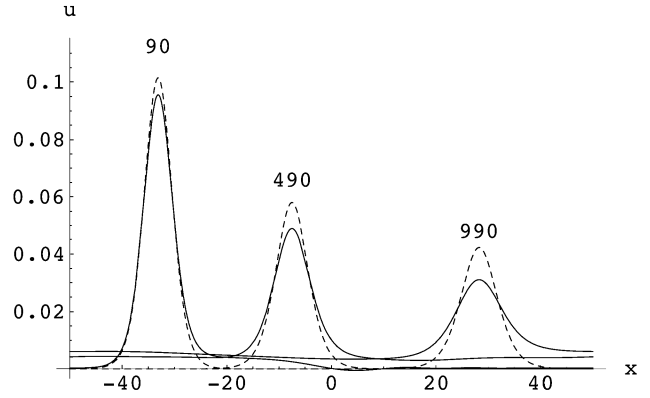

Fig. 6. Decaying soliton (solid curve) with $\kappa = 0.05$, initially at $x = 0$. The dashed curves depict the analytic solitons with the instantaneous velocity of the numeric solitons. The numbers above the peaks indicate the running time, and their particular values have been chosen for illustrative purposes. The soliton has in fact wrapped around the periodic lattice more than 9 times during the time interval of the simulation.

For several reasons, this agreement is necessarily only approximate. First, some time is required for the soliton profile to adjust to the exact form corresponding to its instantaneous velocity. Obviously, only a limited time is available for this adjustment in the presence of dissipation. More importantly, the time independence of the spatial integral of u is not affected by the inclusion of dissipation. Thus, $u(x,t)$ approaches a constant value for all x as $t \to \infty$. On a periodic lattice, as here, this constant is non-zero. This effect is clearly seen in fig. 6, and it is obviously not included in the analytic form of eq. (11) valid in infinite space. Figure 6 shows no indication of the catastrophic break-up of the soliton into small-amplitude waves which might be anticipated in the presence of strong dissipation. The fact that nerve pulses change only little over distances 20 times the pulse width and the small dissipation of heat in the experiment on nerves [9] imply that the magnitude of dissipation is small compared to the values considered here.

4 Collision of pulses

The received wisdom in neuroscience is that action potentials are blocked upon collision [34]. However, compelling evidence for this is not easily found in the literature. The FitzHugh-Nagumo model [35,36], which is a simplified mathematical representation of the Hodgkin-Huxley model, allows for both the cancellation and penetration of pulses depending on parameters [37].

In order to study this aspect, we investigated the head-on collision of two solitary pulses with identical amplitudes and opposite velocities. Our model is based on adiabatic and reversible physics with no detailed mechanism for dissipation other than the inclusion of viscous friction as in

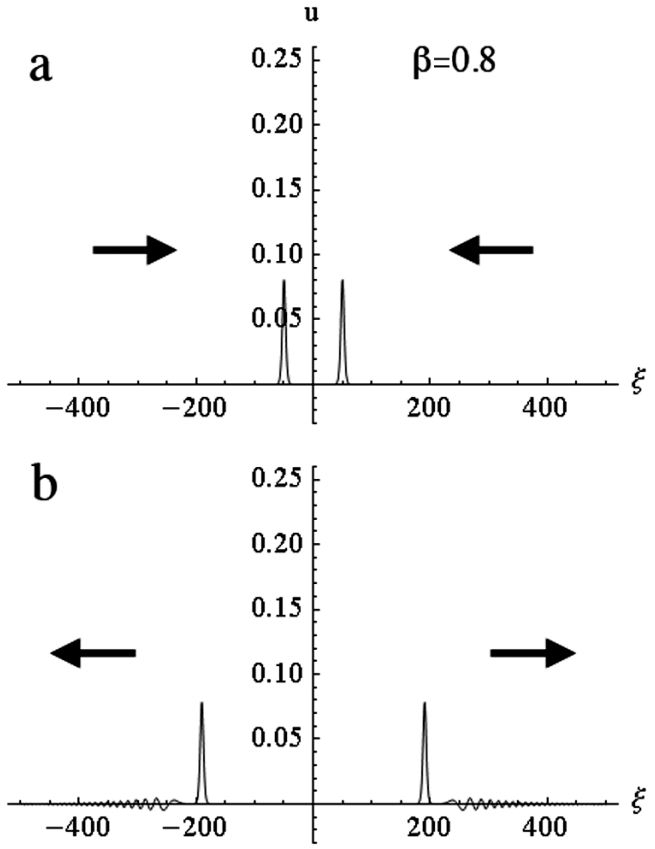

Fig. 7. Collision of two solitons before (a) and after collision (b) shown for $\beta = 0.8$. One obtains small-amplitude noise traveling ahead of the post-collision pulses for $\beta = 0.8$ that carries a very small fraction of the overall energy. The same was found for solitons of different velocity and amplitude.

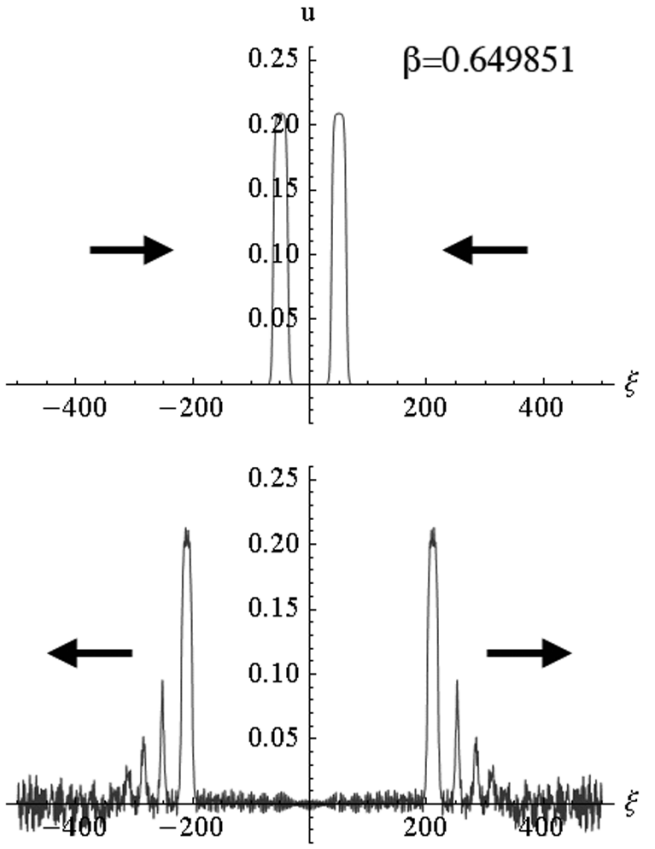

Fig. 8. Collision of two solitons before (top) and after collision (bottom) for $\beta = 0.649850822$ (close to maximum amplitude) and the additional condition of a maximum density change of $u = 0.25$. The pulse falls apart into several solitary peaks with different amplitude and velocity, and some small-amplitude noise.

sect. 3.3. Here, we investigate collisions in the absence of friction. Figure 7 shows the two identical solitons with $\beta = 0.8$ before and after collision. Small-amplitude noise travels ahead of the post-collision pulses and amounts to a very small energy compared to that of the solitary pulses ($\ll 1\%$). The same was found for solitons with other velocities and amplitudes.

The functional dependence of the sound velocity on density is given by eq. (6). It represents a quadratic approximation to the experimental data and yields a satisfactory description in the density regime between solid and liquid membrane state [2]. It is sufficient for the study of those pulse properties considered so far. However, eq. (6) allows the density transiently to exceed the density of the solid phase ($u \approx 0.25$) when large-amplitude pulses collide. Since we regard this as unphysical, we have introduced a "soft barrier" at the density of the solid phase:

$$B(u) = (1 + B_1 u + B_2 u^2)(1 + \mathrm{e}^{\alpha(u-u_{\max})}). \qquad (18)$$

This modification of eq. (6) is only relevant at the moment of collision of two large-amplitude solitons. We used $\alpha = 100$ and as maximum density $u_{\max} = 0.26$, which is close the maximum change of density for the particular membrane discussed here. The result of such a collision of two solitons with β close to the minimum velocity β_0, given by eq. (9), is shown in fig. 8. The soliton falls apart into a sequence of solitons and some additional low-amplitude noise. The closer one is to the minimum velocity, the more pronounced this effect is. Such a decomposition into several pulses was not seen in the absence of this soft barrier. We compared the energy of the largest pulse after the collision with the energy before the collision (fig. 9). See ref. [2] for the calculation of the energy. It can be seen that even for the near-limiting case the fraction lost into smaller solitons and small-amplitude noise is small (*e.g.*, $< 4\%$ for the most extreme case studied). Thus, we see that most of the energy of the major soliton is conserved in collisions even when a maximum density is enforced.

5 Conclusions

We have considered here a number of tests of the stability of the solitons associated with the modified Boussinesq equation, eq. (5). After finding the analytic form of these

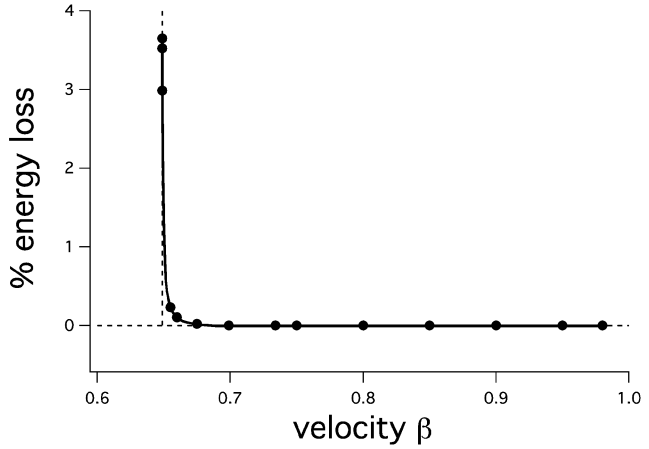

Fig. 9. Loss of soliton energy after collision in %. Compared are the energy content of the largest pulse after collision with the pulse before the collision. Dissipation becomes significant only when the pulses reach their maximum amplitude and minimum velocity.

solitons, we turned to a numerical investigation (with periodic boundary conditions) of the their stability with respect to various perturbations. These solitons were found to be stable with respect to the "smallest possible" perturbations inevitably induced by the finite size of the numerical mesh and to finite but small periodic perturbations. Solitons are found to be produced by arbitrary localized but non-solitonic initial excitations. We have shown that solitons retain their characteristic properties even in the presence of relatively strong dissipation. It was argued in ref. [2] that the measured compression moduli of lipids of biological membranes are suitable for the production of solitons. Finally, in the context of our model, pulses pass through each other "almost undisturbed" with the generation of only small amounts of small-amplitude noise. If a maximum density is introduced, as seems reasonable for the crystalline lipid matrix, large-amplitude solitons can decay into a series of solitons. However, even under these extreme conditions, the bulk of the energy remains in the maximum-amplitude soliton. Thus, our model does not offer a description of the cancellation of pulses suggested by some of the biology literature [34].

These findings may be of immediate relevance for the propagation of the action potential in nerve axons [2]. The solitons described above are subject to friction and dissipation. Nerve membranes are not homogeneous, *i.e.*, they vary both in thickness (*e.g.*, at the site of the soma) and in the specific composition of lipids and proteins. Elastic constants may therefore vary locally. In the present paper we have shown that neither noise nor dissipation affect the propagation of solitary waves as such but rather lead only to slight changes in amplitude and velocity. These pulses are therefore likely to be robust with respect to the unavoidable variance in shape and composition of biological membranes and to dissipative hydrodynamic processes which accompany the observed thickness changes in nerves [38]. Thus, the present results suggest that a model of nerve pulses as *stable* solitary waves is viable even in a realistic physiological environment and that such a model may provide an immediate and reliable explanation of associated mechanical [38] and thermodynamic [7–9] effects that remain unexplained in the presently accepted Hodgkin-Huxley model [1].

Appendix A. Derivation of the viscous friction term used for the evaluation of dissipation in sect. 3.3

In one dimension (x) the Navier-Stokes equations for compressible fluids are

$$\rho\left(\frac{\partial v}{\partial t}+v\frac{\partial v}{\partial x}\right)=-\frac{\partial p}{\partial x}+\eta\frac{\partial^2 v}{\partial x^2}\,,\qquad \frac{\partial \rho}{\partial t}=-\frac{\partial(\rho v)}{\partial x}\,, \tag{A.1}$$

where $v(x,t)$ is the velocity field and $\rho(x,t)$ the density field. The pressure field p is assumed to obey a barotropic constitutive equation, $p=p(\rho)$, and depends indirectly on x and t through ρ. The viscosity η is assumed constant, although it does not change much if it depends on ρ. These equations may also be taken to describe longitudinal unidirectional waves in materials of any dimension n. In that case the viscosity should be taken as a combination of shear and bulk viscosities for the fluid: $\eta=2\eta_{\rm shear}(1-1/n)+\eta_{\rm bulk}$. We shall mainly think of two-dimensional membranes where the density is measured in units of mass per unit of area and $\eta=\eta_{\rm shear}+\eta_{\rm bulk}$.

Using that

$$\frac{\partial(\rho v)}{\partial t}+\frac{\partial\left(\rho v^2\right)}{\partial x}=\rho\left(\frac{\partial v}{\partial t}+v\frac{\partial v}{\partial x}\right), \tag{A.2}$$

we may rewrite these equations as mass and momentum balance

$$\frac{\partial \rho}{\partial t}=-\frac{\partial(\rho v)}{\partial x}\,,\qquad \frac{\partial(\rho v)}{\partial t}=-\frac{\partial M}{\partial x}\,, \tag{A.3}$$

where

$$M=p+\rho v^2-\eta\frac{\partial v}{\partial x}\,. \tag{A.4}$$

Combining the balance equations we get

$$\frac{\partial^2\rho}{\partial t^2}=\frac{\partial^2 M}{\partial x^2}\,, \tag{A.5}$$

which has the basic form of a standard wave equation (if M is linear in ρ).

Assuming that the second term in M is negligible, and that the last term is small, we get in the leading approximation

$$\frac{\partial^2\rho}{\partial t^2}=\frac{\partial}{\partial x}\left(c^2\frac{\partial\rho}{\partial x}\right)+\nu\frac{\partial^2}{\partial x^2}\frac{\partial\rho}{\partial t}\,, \tag{A.6}$$

where $\nu=\eta/\rho$, and where we have introduced $c^2=\partial p/\partial\rho$, and used the equation of continuity to eliminate v. Finally, adding the *ad hoc* dispersive term, we arrive at eq. (3), now including dissipation.

References

1. A.L. Hodgkin, A.F. Huxley, J. Physiol. **117**, 500 (1952).
2. T. Heimburg, A.D. Jackson, Proc. Natl. Acad. Sci. U.S.A. **102**, 9790 (2005).
3. T. Heimburg, A.D. Jackson, Biophys. Rev. Lett. **2**, 57 (2007).
4. T. Heimburg, A.D. Jackson, in *Structure and Dynamics of Membranous Interfaces*, edited by K. Nag (Wiley, 2008) pp. 317–339.
5. S.S.L. Andersen, A.D. Jackson, T. Heimburg, Progr. Neurobiol. **88**, 104 (2009).
6. E. Villagran Vargas, A. Ludu, R. Hustert, P. Gumrich, A.D. Jackson, T. Heimburg, Biophys. Chem. **153**, 159 (2011).
7. B.C. Abbott, A.V. Hill, J.V. Howarth, Proc. R. Soc. London, Ser. B **148**, 149 (1958).
8. J.V. Howarth, R. Keynes, J.M. Ritchie, J. Physiol. **194**, 745 (1968).
9. J.M. Ritchie, R.D. Keynes, Q. Rev. Biophys. **392**, 451 (1985).
10. Y. Kobatake, I. Tasaki, A. Watanabe, Adv. Biophys. **208**, 1 (1971).
11. A. Blicher, K. Wodzinska, M. Fidorra, M. Winterhalter, T. Heimburg, Biophys. J. **96**, 4581 (2009).
12. B. Wunderlich, C. Leirer, A. Idzko, U.F. Keyser, V. Myles, T. Heimburg, M. Schneider, Biophys. J. **96**, 4592 (2009).
13. K. Wodzinska, A. Blicher, T. Heimburg, Soft Matter **5**, 3319 (2009).
14. T. Heimburg, Biophys. Chem. **150**, 2 (2010).
15. J. Gallaher, K. Wodzinska, T. Heimburg, M. Bier, Phys. Rev. E **81**, 061925 (2010).
16. T. Heimburg, A.D. Jackson, Biophys. J. **92**, 3159 (2007).
17. J. Boussinesq, J. Math. Pures. Appl. **7**, 55 (1872).
18. P.G. Drazin, R.S. Johnson, *Solitons: An Introduction* (Cambridge University Press, 1989).
19. N.J. Zabusky, M.D. Kruskal, Phys. Rev. Lett. **15**, 240 (1965).
20. R.V. Mishmash, L.D. Carr, Phys. Rev. Lett. **103**, 140403 (2009).
21. H.-B. Braun, J. Kulda, B. Roessli, D. Visser, K.W. Krämer, H.-U. Güdel, P. Böni, Nature Phys. **1**, 159 (2005).
22. R. Meppelink, S.B. Koller, J.M. Vogels, P.P. van der Straten, E.D. van Ooijen, N.R. Heckenberg, H. Rubinsztein-Dunlop, S.A. Haine, M.J. Davis, Phys. Rev. A **80**, 043606 (2009).
23. B. Damski, W.H. Zurek, Phys. Rev. Lett. **104**, 160404 (2010).
24. J.E. Bjorkholm, A. Ashkin, Phys. Rev. Lett. **32**, 129 (1974).
25. C.-J. Chen, P.K.A. Wai, C.R. Menyuk, Opt. Lett. **17**, 417 (1992).
26. C. Conti, G. Ruocco, S. Trillo, Phys. Rev. Lett. **95**, 183902 (2005).
27. S. Yomosa, Phys. Rev. A **27**, 2120 (1983).
28. C.T. Zhang, Phys. Rev. A **35**, 886 (1987).
29. J.H. Ipsen, G. Karlström, O.G. Mouritsen, H. Wennerström, M.J. Zuckermann, Biochim. Biophys. Acta **905**, 162 (1987).
30. T. Heimburg, Biochim. Biophys. Acta **1415**, 147 (1998).
31. S. Halstenberg, T. Heimburg, T. Hianik, U. Kaatze, R. Krivanek, Biophys. J. **75**, 264 (1998).
32. W. Schrader, H. Ebel, P. Grabitz, E. Hanke, T. Heimburg, M. Hoeckel, M. Kahle, F. Wente, U. Kaatze, J. Phys. Chem. B **106**, 6581 (2002).
33. W.H. Press, S.A. Teukolsky, W.T. Vetterling, B.P. Flannery, *Numerical Recipes in C*, second edition (Cambridge University Press, 1997) Chapt. Random Numbers, pp. 274–283.
34. I. Tasaki, Biochim. Biophys. Acta **3**, 494 (1949).
35. R. FitzHugh, Biophys. J. **1**, 445 (1961).
36. J. Nagumo, S. Arimoto, S. Yoshizawa, Proc. IRE **50**, 2061 (1962).
37. M. Argentina, P. Coullet, V. Krinsky, J. Theor. Biol. **205**, 47 (2000).
38. K. Iwasa, I. Tasaki, R.C. Gibbons, Science **210**, 338 (1980).